International Journal of Environmental Sciences

Full Length Research Article

Effects of Two Earthquakes on Aerosol Characteristics and size distribution over Rajkot, India

Pooja Bhimajiyani, Nimit Godhani, Chintan Jethva and H.P. Joshi
Department of Physics, Saurashtra University, Rajkot-360005, India

ARTICLE INFORMATION

ABSTRACT

The impact of two earthquakes in April & November 2013 on the aerosol characteristics over Rajkot has been studied using satellite observations and ground-based measurements. Two Earthquake events have been analyzed during the study period with average values of Aqua-MODIS AOD at 550 nm, MWR AOD at 6 different wavelengths, Microtops-II AOD at 4 different wavelengths over Rajkot. The first event occurred on 17[th]April 2013, higher AOD values were observed ~0.95using MWR at 380nm wavelength, 0.78 using Microtops-II at 500nm wavelength, and 0.93 using Aqua-MODIS at 550nm, as compared to their normal values of 0.31, 0.45, and 0.45 respectively on control days. The second event was observed on the earthquake of the 15[th]November 2013 with corresponding values of AOD 1.54, 0.80, and 0.76 respectively, as compared to their normal values of MWR (at 380 nm), Microtops-II (at 500 nm), and Aqua-MODIS (at 550 nm) 0.55, 0.47 and 0.43 respectively on control days. Higher particulate matter (PM) concentration of around 19.4, 100.1, and 354.6µg/m^{-3}for PM_1, $PM_{2.5}$, and PM_{10}were found respectively on the first event (i.e. 17 April 2013) which are significantly higher compared to mean values 12.4, 43.7 and 127.8µg/m^{-3} respectively on normal days of April. Corresponding higher values of PM_1, $PM_{2.5}$, and PM_{10}were observed 78.0, 96.5, and 244.8µg/m^{-3}on the second event occurred on 15 November 2013 as compared to their mean values 52.4, 66.4 and 161.4 µg/m^{-3}on control days of November. A significant difference in the size distribution has also been observed during earthquake events as compared to the normal days.

Introduction

Solid or liquid phase particles suspended in the atmosphere are called aerosols. Particles in the atmosphere arise from natural sources as well as anthropogenic activities. Natural sources, such as volcanic activity, produce synoptic-scale effects; while other sources, such as windblown dust, sea-spray, convective, and general circulations produce regional-scale effects in modulating background aerosols. Anthropogenic sources such as industrial pollution, transportation, and biomass combustion are generated locally. On a global scale, the natural sources of aerosols are more important than the anthropogenic aerosols, but regionally anthropogenic aerosols are more important (Kaufman and Fraser, 1983; Ramanathan et al., 2001). Aerosols produce a variety of atmospheric effects. In the lower troposphere, they are important in the formation of fog, mist, and clouds, besides affecting visibility, whereas in the upper regions they produce chemical and electrical effects. These effects are the result of aerosol interaction with radiation. Hence the global studies on the properties of the aerosols are of great importance. Aerosols generated at one place are transported over long distances by the wind systems and they produce consequent effects at locations much farther away from the source. The transport of desert dust

from Asia to the North Pacific atmosphere is well documented by (Husar et al., 1997). Reports of successive outbreaks of extremely dusty air from the Saharan desert with high turbidity and strong attenuation of solar irradiance are observed each year in Cairo and Alexandria, Egypt (Sabbah et al., 2001).

Atmospheric aerosols have been studied using various techniques and instruments, either using ground-based measurements or through remote sensing because of their wide size range and the complexity in the physical and chemical properties. No single method is capable of providing complete information on the aerosol system. Composition and size distribution are fundamentally the most important properties of atmospheric aerosols as far as their indirect effects are concerned (Houghton et al., 2001). Monitoring AOD at different wavelengths is useful for deriving additional information on the size distribution of particles.

The sources and sinks of aerosols are so varied and distributed over the globe, that their physical properties and optical effects show distinct variation with geographic locations. Properties of aerosols in varied environments in India like microphysical

properties at the tropical coastal station Trivandrum (Beegum et al., 2009), temporal and spectral characteristics of aerosol optical depth at Anantapur, a semi-arid region (Kumar et al., 2009),and dust storm effects on aerosol characteristics over Patiala, Northwestern India (Sharma et al., 2012)have been reported. The aerosol parameters after the great Gujarat earthquake (M 7.7) occurred on 26th January 2001 over the Gujarat coast using SeaWiFS data have been studied by (Okada et al., 2004). Anomalous changes in water vapour column in response to the Gujarat earthquake has been reported by(Dey et al., 2004).

In this communication, the effects of two earthquakes on the characteristics of aerosol at the semi-arid location of Rajkot in western Indiawhich occurred near Pakistan, are presented using observations from different instruments such as MICROTOPS-II, MWR, and satellite-based Aqua-MODIS data. Also, the change in PM concentration using Portable Aerosol Spectrometeris reported. On 17 April 2013 (Event-1) earthquake with M 5.6 occurred at the Iran-Pakistan Border (28.11°N 62.35°E). The 15 November earthquake with M 4.9 occurred at 29.83°N 67.50°E (Pakistan).To our knowledge, there is no reported study of earthquake effects on aerosols. Objective of the present study is to evaluate the changes in atmospheric AOD during a special event such as earthquakes.

Materials and methods

Site of observation

The present study area represents a mixture of mineral (dust) and marine aerosols because of its proximity to Rajasthan deserts and the Arabian Sea respectively (Ranjan et al., 2016, 2007). The observations were taken at the Department of Physics in the campus of Saurashtra University, Rajkot (22°18' N, 70°44' E and 142 m above sea level), in Gujarat, western India. The Saurashtra University is situated at Rajkot near the Arabian Sea. The site is a semi-arid urban region free from major industries. Good mixtures of minerals and marine aerosols are expected over this location. Therefore knowledge of the characteristics of aerosols over this location is important for the regional modeling of aerosol.

The climatology of the region is semi-arid that experiences four seasons, winter (December-February), pre-monsoon (March-May), monsoon (June-September), and post-monsoon (October-November), with varying temperature, wind direction, humidity levels, aerosol types, and an average rainfall of ~ 600 mm occurring mostly in the monsoon season. Frequent hazy, fog and pollution-smog conditions occur during winter months which results in reduced visibility.

Instrumentation

Sun Photometer Measurements

Two handheld Solar Light portable Microtops-II (version 2.43 and 5.5) were used in the present study to measure the spectral AOD at four different wavelengths, namely, 500,675,870, and 1020 nm. The Microtops-II has inbuilt sensors to measure pressure and temperature with GPS connectivity which can be useful to obtain the position and time coordinates. The details about the design, calibration, performance, and errors of Microtops-II are described in(Badarinath et al., 2007; Morys et al., 2001; Porter et al., 2001). The measurement technique is based on the principle of measuring the intensity of incoming

solar radiation at particular wavelengths and converted into optical depth using its internal calibration and Langley method(Morys et al., 2001). The irradiance signal (in mV) at different wavelengths is multiplied with the calibration factor (in $Wm^{-2}mV^{-1}$) and the absolute irradiance is obtained in Wm^{-2}.The combined effects of uncertainty in calibration, atmospheric pressure, total ozone amount, and so forth, resultingin total uncertainty in the computed spectral AODs of ~ 0.01-0.025, which is spectrally dependent with highererrors in the UV (Porter et al., 2001). The sun photometric observationswere regularly carried out at Rajkotforclear skyconditions from local sunrise to sunset.

Multi-Wavelength Solar Radiometer (MWR) Measurements

MWR has been in operation at Saurashtra University, Rajkot under collaboration between SPL, VSSC, Trivandrum, and Saurashtra University, as a part of the ARFI project. MWRmakes continuous measurements of direct solar flux at 10 different wavelength bands centred at 380, 400, 450, 500, 600, 650, 750, 850, 935, and 1025nm (with a full width at half maximum bandwidth of 5-6nm and field of view of 2°). The details of the instrument and method of analysis are discussed earlier in detail by several investigators(Gogoi et al., 2014; Kompalli et al., 2010; Moorthy et al., 2007). Out of these 10 wavelengths, 6 wavelengths have been used for the study due to some uncertainty in the data of the other wavelengths.

Description of an Algorithm to analyze MWR data

In the present study,AOD is calculated from the Langley regression method, based on linear regressions of the log of the measured irradiance versus air-mass, computed on a twice-daily basis(Koontz et al., 2013).

Total optical depth (TOD) can be calculated using the equation,

$$TOD_{(t)} = \left(\tau_{\text{Rayleigh}} + \tau_{\text{aerosol}} + \tau_{\text{gas}}\right) = -\frac{1}{am}log\left[\frac{V(\lambda,t)}{V_0(\lambda)}\right]$$

(1)

In this equation gas correction is negligible. By doing Rayleigh correction we can get AOD by subtracting τ_{Rayleigh} from TOD.A network of Multi-Wavelength Radiometer (MWR) stations has been set up at different locations under ARFI project to cover different types of environments; e.g., rural, urban, coastal, marine, arid, desert, etc.

MODIS data

MODIS (Moderate Resolution Imaging Spectroradiometer)on-board polar-orbiting NASA's Earth Observing System (EOS). It's Terra and Aqua satellite provides daily global data of aerosol characteristics using 36 spectral bands ranging from visible to thermal infrared (0.41–14.38 μm), with spatial resolutions of 1000 m, 500 m, and 250m (pixel size at nadir) (Levy et al., 2007). These data sets wereused for aerosol retrievals over landsusing separate algorithms with retrieval uncertaintyof±0.05 ± 15% over land(Levy et al., 2010).For this study, collection 5 (C005) Level 3 Aqua-MODIS AOD at 550nm were obtained for pixel centred over Rajkot on the Earthquake days as well as pre and post-Earthquakedays from NASA website (http://giovanni.gsfc.nasa.gov/).The level 3 daily mean AOD

retrievals (spatial resolution of 1°× 1°) wereused for the observation site.

Portable Aerosol Spectrometer (GRIMM) Measurements
It is used for the continuous measurement of surface aerosols. It measures particle number concentration and particle mass distribution for 31 different size channels ranging from 0.25 to 32 μm usinga light-scattering principle. The measurements of PM_1, $PM_{2.5}$, and PM_{10} which are directly linked to their potential for causing health problems are analyzed to study their variation during such events.

Method of analysis
Aerosol size distribution
From wavelength measurements of the directly transmitted solar flux density as a function of solar zenith angle, one can obtain spectral values of the particulate (Mie) optical depth (King et al., 1978; Shaw, 1976).

(King, 1982; King et al., 1978)described the method of calculating aerosol size distribution (ASD) using the following inversion schemewhich connects the AOD and ASD as

$$\tau_a(\lambda) = \int_0^\infty \pi r^2 Q_{ext}(r, \lambda, m)n_c(r)dr \qquad (2)$$

where r is the particle radius, λ is the wavelength of incident radiation, m is the complex refractive index of aerosol particles, $Q_{ext}(r, \lambda, m)$is the Mie extinction efficiency parameter, $n_c(r)$is the columnar aerosol size distribution, which is the number of particles per unit area per radius interval in a vertical column through the atmosphere.The complex refractive index is the real quantity, represents contribution due to particulate scattering and the imaginary quantity denotes the particles of absorption. For the present analysis,the value of imaginary component m isvery small for the aerosol particles so it is assumed to be negligible.

To separate $n_c(r)$ into two parts as$n_c(r) = h(r).f(r)$,a numerical approach is followed, in which$h(r)$is rapidly varying function with *r* and $f(r)$is slowly varying function. So the above equation can be written as,

$$\tau_a(\lambda) = \sum_{j=1}^q \int_{r_j}^{r_{j+1}} \pi r^2 Q_{ext}(r, \lambda, m)h(r)f(r)dr$$
$$(3)$$

In equation (3) the quadrature error will be less if $f(r)$is assumed to be constant. So that a system of linear equations results, which may be written as,
$$\tau_a(\lambda) = Af(r) + \varepsilon \qquad (4)$$

Where$A = \int \pi r^2 Q_{ext}(r, \lambda, m)h(r)dr$ and ε is an error that arises due to the deviation between the measured $\tau_a$and theoreticalτ_a.

Junge exponent(ν) is computed from the wavelength dependence of AOD,where $v = \alpha + 2$and used as a zero-order weighting function $h^0(r)$ as an initial guess, the first-order f^1 values are evaluated using the equation,

$$f^{(1)} = (A^T S_\varepsilon^{-1} + \gamma H)^{-1} A^T S_\varepsilon^{-1} \tau_m \qquad (5)$$

Where; H is a mean diagonal matrix, γ is a non-negative Lagrangian multiplier, and S_ε is the measured covariance matrix, and superscript T indicates matrix transposition. This iteration procedure is done repeatedly till the observed value τ_a comes closer to the re-computed τ_a.

According to (Moorthy et al., 1991) size distribution can be broadly classified into three groups according to their shape; viz., the modified Judge type (MJ), the unimodal (UM) distribution. The MJ distribution is characterized by a nearly flat region at lower particle sizes with the number density decreasing slowly with an increase in particle radius. The UM type shows a pronounced mode at some value of the radius with the aerosol content falling off on either side of the mode. The third type,bimodal (BM) is characterized by a secondary mode occurring at a fairly large value of r while the primary mode does not appear explicitly.

Results
During this study period, two Earthquake events occurred near the study region. The first event occurred on 17 April 2013 at the Iran-Pakistan border (28.11°N 62.35°E)around 8:45 am (LT) with *M* 5.6. The second event occurred on 15 November 2013 at 29.83°N 67.50°Earound 04:12 pm (LT) with *M*4.9.

AOD variation
The change in AOD variation using MWR, Microtops-II, and Aqua-Modis are shown in Table 1 at different wavelengths for both the events. Increased AOD was observed at all the wavelengths on the earthquake day for both the events as compared with the previous days of the events. The peak in AOD value was observed as high as 0.85 and 0.78 at 500 nm using MWR and Microtops-II observations and 0.93 at 550 nm using satellite observation of Aqua-MODIS.

Table 1. Daily mean AOD values at different wavelengths using MWR, MICROTOPS, and Aqua-MODIS observations.

Wavelength (nm)	MWR						MICROTOPS				Aqua-MODIS
	380	400	500	600	650	750	500	675	870	1020	550
Event 1											
11-04-2013	0.18	0.17	0.16	0.15	0.14	0.09	0.46	0.43	0.42	0.27	0.42
12-04-2013	0.46	0.36	0.36	0.31	0.30	0.16	0.33	0.28	0.28	0.41	0.57
13-04-2013	0.26	0.20	0.15	0.12	0.11	0.08	-	-	-	-	-

Date	MWR 380nm	400nm	500nm	600nm	650nm	750nm	Microtops 500nm	675nm	870nm	1020nm	MODIS 550nm
14-04-2013							0.37	0.32	0.31	0.25	0.31
15-04-2013	0.20	0.17	0.15	0.15	0.14	0.12	0.38	0.33	0.31	0.30	0.36
16-04-2013	0.40	0.37	0.31	0.29	0.28	0.20	0.34	0.29	0.29	0.28	0.33
17-04-2013	**0.95**	**0.90**	**0.85**	**0.73**	**0.70**	**0.61**	**0.78**	**0.74**	**0.73**	**0.72**	**0.93**
18-04-2013	-	-	-	-	-	-	0.78	0.73	0.71	0.69	0.64
19-04-2013	-	-	-	-	-	-	0.61	0.50	0.46	0.43	0.74
20-04-2013	-	-	-	-	-	-	-	-	-	-	0.46
					Event 2						
11-11-2013	0.53	0.35	0.33	0.29	0.24	0.19	0.65	0.44	0.32	0.27	0.45
12-11-2013	0.58	0.52	0.49	0.37	0.30	0.23	0.52	0.35	0.26	0.24	0.69
13-11-2013	0.78	0.74	0.66	0.46	0.34	0.33	0.55	0.39	0.30	0.26	0.47
14-11-2013	-	-	-	-	-	-	-	-	-	-	0.55
15-11-2013	**1.54**	**1.49**	**1.21**	**1.14**	**0.89**	**0.59**	**0.80**	**0.57**	**0.41**	**0.34**	**0.76**
16-11-2013	-	-	-	-	-	-	-	-	-	-	0.30
17-11-2013	-	-	-	-	-	-	-	-	-	-	0.57
18-11-2013	0.83	0.70	0.57	0.53	0.48	0.20	0.55	0.37	0.28	0.19	0.36
19-11-2013	0.55	0.48	0.36	0.30	0.29	0.12	0.31	0.21	0.17	0.11	0.30
20-11-2013	0.49	0.48	0.46	0.46	0.42	0.30	0.28	0.19	0.17	0.12	0.17

Fig. 1 (a-b) shows the spectral dependence of AOD on days before and on 17th April 2013 when the earthquake was occurred atthe Iran-Pakistan border using MWR and Microtops-II. Fig.1 (c) shows the daily variation of AOD derived using Aqua-MODIS observations at 550 nm. It is observed that on the day before the earthquake, values of AOD at all the wavelengths remain lower below 0.5 – 0.6 but on 17th April 2013 variation in AOD values at all the wavelengths increase drastically. The gradual decrease in AOD was observed on MODIS data shows the settle down of atmospheric aerosols to their normal range. Similarly, Fig. 2 represents the behavior of spectral dependence on the second event of 15th November 2013. It is noted that the background AOD during the November month of 2013 remains higher as compared to April 2013.
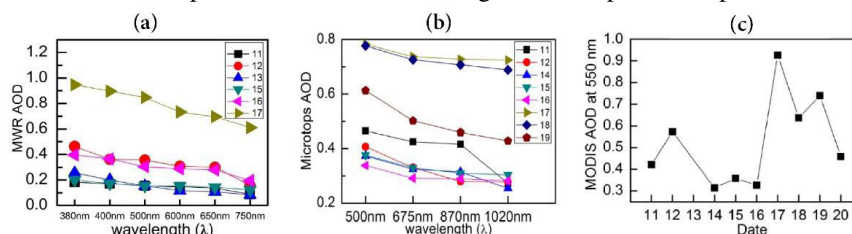
Fig 1. The AOD variation during April 2013 before and after the days of event including the event day at different wavelengths using (a) MWR,and (b) Microtops-II; (c) AOD derived from Aqua-MODIS (at 550 nm) during the same event.
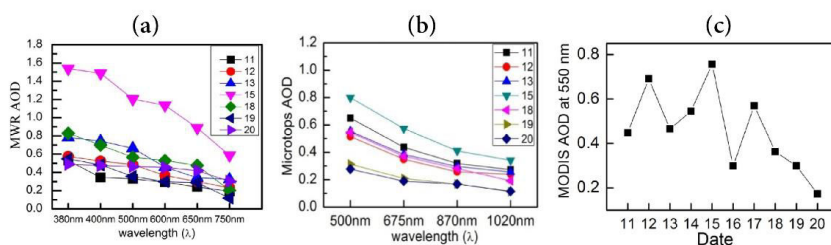
Fig 2. Same as Fig. 1 but for the event of November 2013.

Size distribution
Table-2 shows the variation ofPM$_1$, PM$_{2.5}$, and PM$_{10}$ concentrationfor both the earthquake events. It is observed that on Event-1 (17th April 2013) the PM$_{2.5}$ and PM$_{10}$ concentrations were increased noticeably at the level of 100.1, and 354.6 µg/m^{-3}respectively while PM$_1$ concentration was increased slightly, suggesting the increase in coarse mode abundance during this event. Similar observations were found on the Event-2 (15th November 2013) with increased concentration of PM1, PM2.5, and PM10. It is noted that on Event-2 the values of PM concentration on normal days remain higher as compared to April.

Table 2. The concentration of PM$_1$,PM$_{2.5}$, and PM$_{10}$ using Portable Aerosol Spectrometer.

Date	PM$_1$	PM$_{2.5}$	PM$_{10}$
	Event 1		
11-04-2013	10.9	42.5	106.2
12-04-2013	14.1	58.4	172.5
13-04-2013	09.0	33.1	100.7

15-04-2013	13.3	40.8	113.4
16-04-2013	10.4	35.5	108.9
17-04-2013	**19.4**	**100.1**	**354.6**
18-04-2013	13.4	56.5	204.8
19-04-2013	15.6	39.6	88.7
Event 2			
12-11-2013	50.9	64.2	151.4
13-11-2013	50.9	66.3	154.4
14-11-2013	44.0	52.5	99.6
15-11-2013	**78.0**	**96.5**	**244.8**
16-11-2013	75.7	92.4	228.7
17-11-2013	69.1	85.7	190.1
18-11-2013	40.0	56.4	135.9
19-11-2013	39.0	51.2	154.1
20-11-2013	50.2	62.9	177.1

The size distribution curves derived using inversion of AOD values from MWR at six different wavelengths are analyzed. Fig. 3 shows size distribution during days around the 17th April 2013 event, it is clear that before the earthquake event day size distribution follows the MJ or UM type. On earthquake (17th April 2013) day the columnar number density (*dNc/dlog(r)*) extends downward up to $10^{-1} m^{-2} \mu m^{-1}$ as compared to the days before the earthquake which remains up to $10^{-9} m^{-2} \mu m^{-1}$. This type of curve shows BM type distribution with an increase in coarse mode concentration. Likewise, Fig. 4 shows the size distribution curves around the days of Event-2 (15th November 2013). The BM type size distribution was also observed on the 15th November 2013 earthquake, except other days which shows UM type.
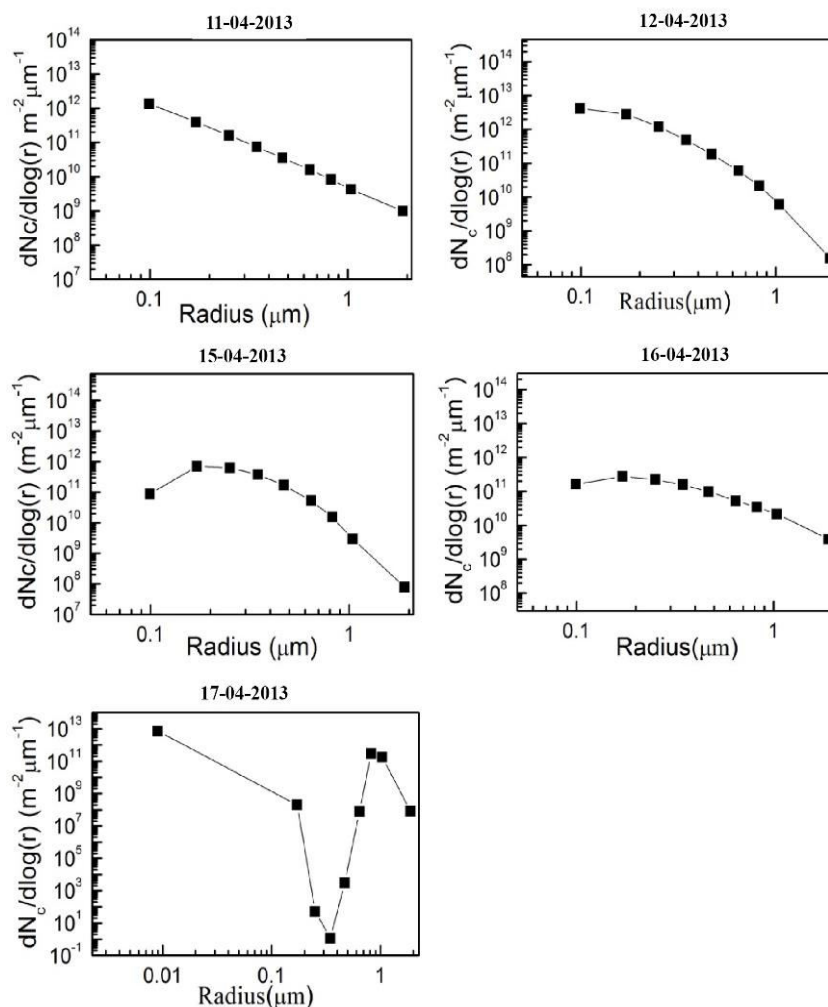
Fig 3. The aerosol size distribution using inversion algorithm around the days of the event on April 2013.
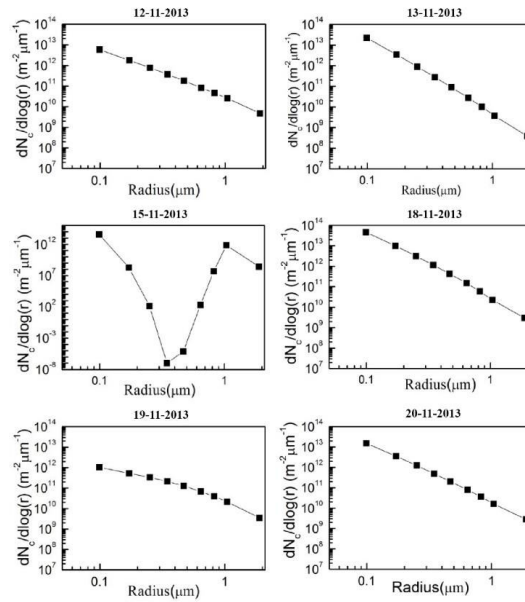
Fig 4. Same as Fig. 3 but for the event of November 2013.

Back Trajectory analysis to determine the source of aerosols
To study whether aerosols are transported on the event days from the origin of an earthquake or not; the 5 days backward wind trajectories are generated using the Hybrid Single-Particle Lagrangian Integrated Trajectory (HY-SPLIT) model of the National Oceanic and Atmospheric Administration (NOAA), United States (available at http://www.arl.noaa.gov/ready/hysplit4.html) for both the events. Fig. 5 (a-b) shows 5-days back trajectories from 17 April 2013 and 15 November 2013 respectively, to locate the path of the dust-carrying air mass at the study region at three altitudes, viz.

500 m, the mixed layer; 1500 m, above the boundary layer where the dust is lifted by convection and transported over a long distance; and 2500 m, the relatively free troposphere. The wind in the mixed layer is responsible for raising the loose soil dust particles in the atmosphere. In the first trajectory wind is coming from Iraq then Iran and from Pakistan before coming to Rajkot at 1500 and 2500 m height. It is noted that wind is coming from the station where the earthquake occurred i.e. Iran-Pakistan border. In the second trajectory, wind direction is similarly located towards North-westerly which is the origin of the second earthquake of November 2013.
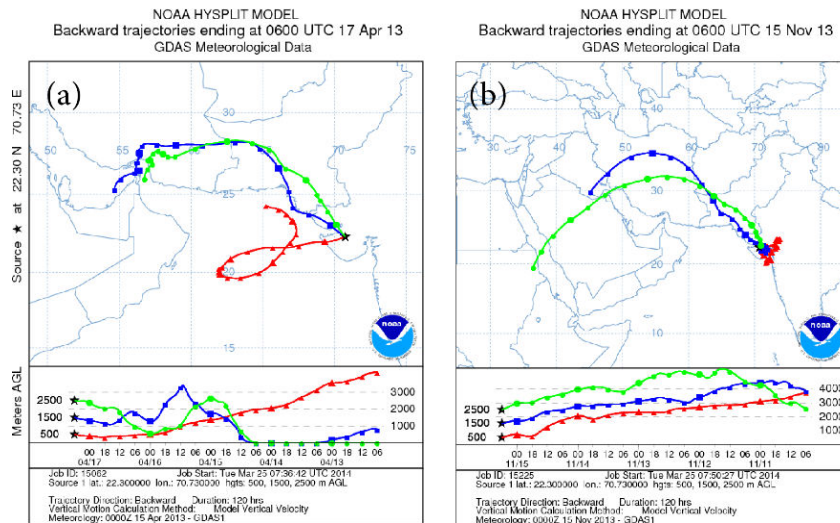
Fig 5: NOAA-HYSPLIT model backward wind trajectory at 500, 1500, and 2500 m altitude from (a) 13-17 April 2013(Event-1)and (b) from 11-15 November 2013 (Event-2) at Rajkot, India.

Conclusion
The variation in aerosol during the twoearthquake events were investigated by comparing ground-based measurements of MWR and Microtops-II, and satellite observations of Aqua-MODIS AOD data at Rajkot location which is a semi-arid urban

region.The first event occurred on 17[th]April 2013, and the second event on 15[th]November 2013. During the study period, an important feature noticed is the higher values of AOD on Earthquake days, and size distribution on these days is unique. The BM type of size distribution is observed on earthquake days

when compared to the non-event days that show the UM type of distribution. The back trajectory of wind confirms the origin of wind parcels from the earthquake location. By studying variation in AOD values using different instruments on the event days, one can conclude that there is the effect of the earthquake on aerosols and aerosol size distribution. This may be a new area of research in terms of aerosol climatology.The measured values of PM concentration using Portable Aerosol Spectrometer at study location also show higher values at PM_1, $PM_{2.5}$, and PM_{10}during earthquake days.

Acknowledgments

References

Badarinath, K., Kharol, S.K., Kaskaoutis, D., Kambezidis, H., 2007. Dust storm over Indian region and its impact on the ground reaching solar radiation—a case study using multi-satellite data and ground measurements. Sci. Total Environ. 384, 316–332.

Beegum, S.N., Moorthy, K.K., Babu, S.S., 2009. Aerosol microphysics over a tropical coastal station inferred from the spectral dependence of Angstrom wavelength exponent and inversion of spectral aerosol optical depths. J. Atmospheric Sol.-Terr. Phys. 71, 1846–1857.

Dey, S., Sarkar, S., Singh, R., 2004. Anomalous changes in column water vapor after Gujarat earthquake. Adv. Space Res. 33, 274–278.

Gogoi, M.M., Moorthy, K.K., Kompalli, S.K., Chaubey, J.P., Babu, S.S., Manoj, M., Nair, V.S., Prabhu, T.P., 2014. Physical and optical properties of aerosols in a free tropospheric environment: Results from long-term observations over western trans-Himalayas. Atmos. Environ. 84, 262–274.

Houghton, J., Albritton, D., Meira Filho, L., Cubasch, U., Dai, X., Ding, Y., Griggs, D., Hewitson, B., Isaksen, I., Karl, T., 2001. Technical summary of working group 1., in: Climate Change 2001: The Scientific Basis. Contributions of Working Group I to the Third Assessment Report of the Intergovernmental Panel on Climate Change. Cambridge University Press.

Husar, R.B., Prospero, J.M., Stowe, L.L., 1997. Characterization of tropospheric aerosols over the oceans with the NOAA advanced very high resolution radiometer optical thickness operational product. J. Geophys. Res. Atmospheres 102, 16889–16909.

Kaufman, Y.J., Fraser, R.S., 1983. Light extinction by aerosols during summer air pollution. J. Clim. Appl. Meteorol. 22, 1694–1706.

King, M.D., 1982. Sensitivity of constrained linear inversions to the selection of the Lagrange multiplier. J. Atmospheric Sci. 39, 1356–1369.

King, M.D., Byrne, D.M., Herman, B.M., Reagan, J.A., 1978. Aerosol size distributions obtained by inversions of spectral optical depth measurements. J. Atmospheric Sci. 35, 2153–2167.

Kompalli, S.K., Babu, S.S., Moorthy, K.K., 2010. Inter-comparison of aerosol optical depth from the Multi-Wavelength Solar Radiometer with other radiometric measurements. Indian J. Radio Space Phys. 39, 8.

Koontz, A., Flynn, C., Hodges, G., Michalsky, J., Barnard, J., 2013. Aerosol optical depth value-added product. U. S. Dep. Energy Wash. DC USA.

Kumar, K.R., Narasimhulu, K., Reddy, R., Gopal, K.R., Reddy, L.S.S., Balakrishnaiah, G., Moorthy, K.K., Babu, S.S., 2009. Temporal and spectral characteristics of aerosol optical depths in a semi-arid region of southern India. Sci. Total Environ. 407, 2673–2688.

Levy, R.C., Remer, L., Mattoo, S., Vermote, E., Kaufman, Y., 2007. Second-generation algorithm for retrieving aerosol properties over land from MODIS spectral reflectance. J Geophys Res 112, D13.

Levy, R.C., Remer, L.A., Kleidman, R.G., Mattoo, S., Ichoku, C., Kahn, R., Eck, T.F., 2010. Global evaluation of the Collection 5 MODIS dark-target aerosol products over land. Atmospheric Chem. Phys. 10, 10399–10420. https://doi.org/10.5194/acp-10-10399-2010

Moorthy, K.K., Babu, S.S., Satheesh, S., 2007. Temporal heterogeneity in aerosol characteristics and the resulting radiative impact at a tropical coastal station? Part 1: Microphysical and optical properties.

Moorthy, K.K., Nair, P.R., Murthy, B.K., 1991. Size distribution of coastal aerosols: effects of local sources and sinks. J. Appl. Meteorol. 30, 844–852.

Morys, M., Mims III, F.M., Hagerup, S., Anderson, S.E., Baker, A., Kia, J., Walkup, T., 2001. Design, calibration, and performance of MICROTOPS II handheld ozone monitor and Sun photometer. J. Geophys. Res. Atmospheres 106, 14573–14582.

Okada, Y., Mukai, S., Singh, R., 2004. Changes in atmospheric aerosol parameters after Gujarat earthquake of January 26, 2001. Adv. Space Res. 33, 254–258.

Porter, J.N., Miller, M., Pietras, C., Motell, C., 2001. Ship-Based Sun Photometer Measurements Using Microtops Sun Photometers. J. Atmospheric Ocean. Technol. 18, 765–774. https://doi.org/10.1175/1520-0426(2001)018<0765:SBSPMU>2.0.CO;2

Ramanathan, V., Crutzen, P.J., Lelieveld, J., Mitra, A., Althausen, D., Anderson, J., Andreae, M.O., Cantrell, W., Cass, G., Chung, C., 2001. Indian Ocean Experiment: An integrated analysis of the climate forcing and effects of the great Indo-Asian haze. J. Geophys. Res. Atmospheres 106, 28371–28398.

Ranjan, R.R., Joshi, H.P., Iyer, K.N., 2007. Spectral Variation of Total Column Aerosol Optical Depth over Rajkot: A Tropical Semi-arid Indian Station. Aerosol Air Qual. Res. 7, 33–45. https://doi.org/10.4209/aaqr.2006.08.0012

Ranjan, R.R., Manani, N.H., Ghadai, N.C., Joshi, H.P., Iyer, K.N., 2016. Seasonal Variations Of Aerosol Optical Depth Over Rajkot: A Semiarid Urban Region In Gujarat, India 3, 5.

Sabbah, I., Ichoku, C., Kaufman, Y.J., Remer, L., 2001. Full year cycle of desert dust spectral optical thickness and precipitable water vapor over Alexandria, Egypt. J. Geophys. Res. Atmospheres 106, 18305–18316.

Sharma, D., Singh, D., Kaskaoutis, D., 2012. Impact of two intense dust storms on aerosol characteristics and radiative forcing over Patiala, northwestern India. Adv. Meteorol. 2012.

Shaw, G.E., 1976. Error analysis of multi-wavelength sun photometry. Pure Appl. Geophys. PAGEOPH 114, 1–14. https://doi.org/10.1007/BF00875487